Widths of ^2S, $^2P^o$, and ^2D resonances in Li I, Be II, and B III

Brian F. Davis

*Department of Chemical and Physical Sciences, University of North Carolina at Wilmington,
Wilmington, North Carolina 28403-3297*

Kwong T. Chung

Department of Physics, North Carolina State University, Raleigh, North Carolina 27695-8202

The autoionization widths of the lower ^2S, $^2P^o$, and ^2D Feshbach resonances in Li I, Be II, and B III are calculated with the saddle-point complex-rotation method. For Be II and B III the radiation widths are also computed. Relativistic and mass polarization corrections to the resonance energy are included. The width results for the $[1s(2s2p)^3P]^2P^o$ and $(1s2p2p)^2D$ states are compared with other theoretical results and with the recently published experimental results for Li I and Be II. Transition wavelengths involving these autoionizing states are also calculated and compared with theory and experiment. Due to the substantial difference between theory and experiment on the Li$[1s(2s2p)^3P]^2P^o$ width, a detailed study is made on the convergence of this width with respect to the closed channel, open-channel target state and out-going electron wave function to access the stability and reliability of the theoretical result.

I. INTRODUCTION

Recently, autoionization widths have been measured for the $[1s(2s2p)^3P]^2P^o$ and $(1s2p2p)^2D$ resonances in Li I (Ref. 1) and Be II (Ref. 2). These have been obtained by analyzing the broadened line profiles resulting from the optical transitions $(1s2p2p)^2P \rightarrow [1s(2s2p)^3P]^2P^o$ and $[(1s2p)^3P3d]^2D^o \rightarrow (1s2p2p)^2D$ which are seen in beam-foil light sources. These radiative transitions are observed because the upper state, although core excited, is metastable against autoionization in the LS-coupling scheme due to conservation of parity (see Fig. 1). These lines are broadened due to the fact that the lower state primarily decays by autoionization. The total width of these lines is the sum of the radiative and autoionization widths of the upper and lower states. In the energy region of interest, the relativistic spin-induced autoionization rates of the upper states are very small. For Li, the radiative widths of the upper and lower states can be neglected with the experimental resolution obtained, however, for the

FIG. 1. Optical transitions recently measured for the core-excited→lower-lying autoioning states. They have been observed for Li I and Be II. The upper states are metastable against autoionization in the LS coupling scheme due to conservation of angular momentum and parity. For Li I and Be II, the widths of the lower state are significantly larger.

$(1s2p2p)^2P \rightarrow [1s(2s2p)^3P]^2P^o$ transition in Be II and B III these widths have a small but non-negligible effect.[2]

In this work we present results for the autoionization widths of the lower ^2S, $^2P^o$, and ^2D resonances of the lithium isoelectronic sequence from $Z=3$ to 5. These results were obtained with the saddle-point complex-rotation method. In an earlier work,[3] this method was tested for a three-electron system by applying it to the $(1s2s2s)^2S$ resonance for $Z=2$ to 5. The complex eigenvalue, $E-i\Gamma/2$, was found to be very stable with respect to the rotation angle and the nonlinear parameter of the scattered electron in the open-channel component. In that work it was mentioned that the various theoretical results for the width of Be II $(1s2s2s)^2S$ were in serious disagreement. In the recent experimental publications,[1,2] it has also been pointed out that large discrepancies exist among the various theoretical results for the widths of the $[1s(2s2p)^3P]^2P^o$ and $(1s2p2p)^2D$ resonances in Li and Be II. It is our hope that calculating the widths of many different states along the isoelectronic sequence will provide more theoretical data to stimulate further experimental measurements and will also help access the reliability of our theoretical method as well as that of the existing experimental techniques.

For the case of the Li $[1s(2s2p)^3P]^2P^o$ width, our result differs substantially from that of the experiment. It is, therefore, worthwhile to look closely into the theoretical calculation for this state. To accomplish this, we examine the stability and convergence of this theoretical result with respect to the wave functions of the closed-channel, open-channel target state as well as that of the outgoing electron. These results will be reported in later sections.

In the past, the calculated resonance energy positions[4-6] were usually compared with observations from Auger spectroscopy where an experimental uncertainty of
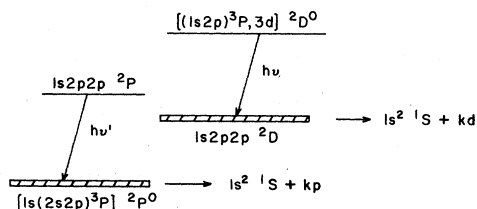
50-100 meV is quoted or with optical-absorption spectroscopy with an experimental uncertainty of 6—20 meV. The results from the saddle-point technique compare well with these experiments. In the recent optical-emission spectroscopy measurements, the transitions of interest are usually observed in the 3000—4000-Å region where an experimental uncertainty of 1 Å corresponds to about 1 meV. This presents a new challenge to the theoretical methods. In order to meet this challenge, we reexamine the nonrelativistic energy calculated before[4-8] by including more correlations and by including the relativistic and mass-polarization corrections. These new results will be compared with those from optical-emission spectroscopy.

II. THEORY AND RESULTS

The nonrelativistic Hamiltonian for the three-electron system in atomic units (a.u.) is given by

$$H_0 = \sum_{i=1}^{3} \left[-\frac{1}{2}\nabla_i^2 - \frac{Z}{r_i} \right] + \sum_{pairs} \frac{1}{r_{ij}} , \quad (1)$$

where Z is the nuclear charge and r_{ij} is the interelectron distance. For a complex-rotation computation[9] the rotated Hamiltonian is obtained by scaling each radial coordinate with $e^{i\theta}$, i.e., r_j becomes $r_j e^{i\theta}$, where θ is the angle of rotation. If we refer to the N-electron radial coordinates collectively as R_N and the corresponding angular variables as Ω_N, then the form of a rotated wave function of ^2L symmetry becomes

$$\Psi(^2L) = \sum_j C_j \phi_j^L(R_3 e^{i\theta}, \Omega_3)$$

$$+ A \sum_k D_k \psi_g(R_2 e^{i\theta}, \Omega_2) U_k^L(\mathbf{r}) \quad (2)$$

where C_j and D_k are linear variation parameters and A is an antisymmetrization operator.

The first term in Eq. (2) represents the closed-channel component. In this term, the ϕ_j^L are optimized, antisymmetrized, configuration interaction basis functions with the "proper"[10] $1s$ vacancy built in. These closed-channel basis functions are obtained from a saddle-point solution for the particular resonance and nuclear charge of interest. That is,

$$\Psi_{sp} = \sum_j B_j \phi_j^L(R_3, \Omega_3, \alpha, q) \quad (3)$$

is obtained by the variation

$$\delta \frac{\langle \Psi_{sp} | H_0 | \Psi_{sp} \rangle}{\langle \Psi_{sp} | \Psi_{sp} \rangle} = 0 . \quad (4)$$

The linear variational parameters B_j and the nonlinear parameter set represented by α are obtained by minimizing the energy, while q, the nonlinear parameter in the $1s$ vacancy orbital is obtained by maximizing the energy with respect to it. For the detailed form of the ϕ_j^L, the interested reader is referred to Ref. 4. The convergence of the saddle-point energy is illustrated for the case of the $[1s(2s\,2p)^3P]^2P^o$ resonance of lithium in Table I. In this table, we give the energy contribution for each partial

TABLE I. Nonrelativistic energy and wave function for the $[1s(2s\,2p)^3P]^2P^o$ state of lithium (in atomic units).

	Partial wave	Number of terms	$-\Delta E$
1	$(s,p)^3P\ s$	18	5.294 313 6
2	$(s,p)^1P\ s$	13	0.007 351 0
3	$(s,s)^3S\ p$	11	0.000 885 0
4	$(s,s)^1S\ p$	7	0.000 394 0
5	$(p,s)^3P\ s$	2	0.000 060 8
6	$(s,p)^3P\ d$	8	0.004 973 1
7	$(s,p)^1P\ d$	7	0.001 582 9
8	$(p,d)^1P\ s$	6	0.001 274 2
9	$(p,d)^3P\ s$	1	0.000 077 2
10	$(p,p)^1S\ p$	5	0.000 817 6
11	$(p,p)^3S\ p$	5	0.000 452 6
12	$(d,f)^1P\ s$	2	0.000 144 7
13	$(d,f)^3P\ s$	1	0.000 112 6
14	$(d,d)^1S\ p$	2	0.000 089 5
15	$(d,d)^3S\ p$	1	0.000 025 6
16	$(f,g)^1P\ s$	2	0.000 034 1
17	$(f,g)^3P\ s$	1	0.000 001 6 7
18	$(g,h)^1P\ s$	1	0.000 010 2
19	$(f,f)^1S\ p$	2	0.000 016 6
20	$(f,f)^3S\ p$	1	0.000 003 1
21	$(p,s)^1P\ s$	2	0.000 008 2
22	$(p,s)^3P\ d$	4	0.000 017 9
23	$(p,s)^1P\ d$	2	0.000 019 6
24	$(s,d)^1D\ f$	2	0.000 035 6
25	$(s,d)^3D\ f$	3	0.000 032 5
26	$(s,f)^1F\ g$	1	0.000 011 9
	Total	110	5.312 760 8

wave along with the number of terms used in that partial wave.

The second term in Eq. (2) represents the open-channel component. ψ_g is the $(1s\,1s)^1S$ two-electron target state. For this state we use a three-partial-wave, eight-term wave function.[3] In Table II the convergence of the energy of this target state for Li II, Be III, and B IV is demonstrated and compared with the nonrelativistic energy of Pekeris.[11] The square integrable basis set used for representing the scattered electron is given by

$$U_k^L(\mathbf{r}) = r^k e^{-\gamma r} Y_L(\Omega) , \quad (5)$$

where γ is a nonlinear variational parameter. In Eqs. (2) and (5) the angular and spin coupling of the target state ψ_g with the U_k^L is suppressed, these functions are coupled to form the ^2L symmetry of interest.

With the Ψ of Eq. (2), the width and the shift from the saddle-point energy are calculated by the standard variation method

$$\delta \frac{\langle \Psi | H_0(\theta) | \Psi \rangle}{\langle \Psi | \Psi \rangle} = 0 . \quad (6)$$

In the preceding procedure the unconjugated $e^{i\theta}$ is used in the complex conjugated wave function. For a more detailed account of the above procedure the interested reader

TABLE II. Convergence of the energy of the three-partial-wave, eight-term $(1s\,1s)^1S$ target state and comparison with Pekeris's value (in a.u.).

	This work				Pekeris (Ref. 11)
No. of partial waves	1	1	2	3	
No. of terms	1	4	7	8	
Li II	−7.222 656	−7.251 861	−7.274 796	−7.276 970	−7.279 913
Be III	−13.597 656	−13.625 239	−13.649 025	−13.651 410	−13.655 566
B IV	−21.972 656	−22.000 695	−22.024 882	−22.027 384	−22.030 972

is referred to Ref. 12.

In Table III we present our results. E_{sp} is the saddle-point energy obtained from Eq. (4). L is the total number of angular and spin partial waves and N is the total number of basis functions used in the calculation of E_{sp}. The column labeled q gives the optimized value of the non-linear parameter in the $1s$ vacancy orbital,

$$\phi_{1s} = Ce^{-qr} \qquad (7)$$

where C is a normalization constant. It is interesting to note that $q \simeq Z - \frac{1}{2}$, indicating that the $1s$ vacancy orbital is approximately half shielded from the nucleus by the $1s$ electron. The results tabulated under the headings $\langle H_1 + H_2 \rangle$ (correction to the kinetic energy and Darwin term), $\langle H_3 \rangle$ (contact term), H_4 (retardation), and H_5 (mass polarization) are obtained by calculating the expectation value of the appropriate operator with the saddle-point wave functions. The explicit form of these operators is given in Ref. 3. We note that the relativistic and mass polarization corrections vary smoothly as a function of nuclear charge.

In the complex-rotation computation [Eq. (6)], the inclusion of 15 terms in the open channel [i.e., k runs from 0 to 14 for ^2S states, 1 to 15 for $^2P^o$ states, and 2 to 16 for ^2D states in Eq. (2)] yields a converged complex energy, $E_r - i(\Gamma/2)$. This energy is stable with respect to the rotation angle θ, and the nonlinear parameter, γ, as has been demonstrated in Ref. 3. In order to keep the size of the complex matrix reasonable for diagonalization we restrict the number of angular partial waves used in the closed-channel component to thirteen. For states with more than thirteen partial waves in the closed channel, we eliminate the less important ones. For example, the complex-rotation calculation for Li$[1s\,(2s\,2p)^3P]^2P^o$ is done using only the first thirteen partial waves in Table I.

The value of E_r in the complex energy turns out to be shifted by a small amount from the corresponding saddle-point energy. This results from the interaction of the closed- and open-channel components of the total wave function through the Hamiltonian. This shift from the saddle-point energy is defined by

$$\Delta = E_r - E_{\text{sp}} \qquad (8)$$

and is given in Table III. If partial waves are eliminated

from the closed-channel component in the calculation of E_r, then the corresponding result for E_{sp} is used to compute Δ. Δ is positive for most cases, however, for a few states (see Table III) it is negative and small. This shift usually depends on the accuracy of the closed-channel basis functions used in Eq. (6). The small shifts shown in the table seem to justify the inner shell vacancy picture which is the foundation of the saddle-point technique.

The resonances given in Table III are the lowest resonance levels for a given angular symmetry. For this reason some of the lithium resonances are omitted. For instance the $(1s\,2p\,2p)^2S$ resonance in Li appears as a much higher root than the second in the secular equation. The $[(1s\,2s)^1S\,3p]^2P^o$ state of Li is the seventh lowest $^2P^o$ resonance. This state acts as a perturber in the $[(1s\,2s)^3S\,np]^2P^o$ series.[6] The $[(1s\,2s)^1S\,3d]^2D$ state of Li lies in the inelastic scattering energy region,[6] it is not considered in this work. The $1s\,2s\,2s\,^2S$ states have been published earlier,[3] they are not included in Table III.

Γ_e and Γ_r in Table III are the widths due to autoionization and dipole radiative transitions, respectively. Γ_e is obtained by taking twice the imaginary part of the complex energy resulting from Eq. (6). Γ_r is calculated by computing the transition probabilities from the resonance level of interest to the more important lower autoionizing and bound states. The Γ_r for Be II are from an earlier work.[8] To illustrate the various contributions to Γ_r for B III we tabulate the transition probabilities (in units of sec^{-1}) from the $^2P^o$ resonances to the lower states in Table IV. The conversion factor necessary to convert these results into atomic units of energy is 4.13393×10^{16} sec·a.u. The radiative widths of the lithium resonances are small. They are not calculated in this work.

It has been remarked[2] that autoionization widths for a given resonance should be essentially independent of variations in Z. This argument is based on a computation[13] of the transition probability (via the $1/r_{ij}$ interelectron repulsion perturbation) between initial- and final-state wave functions that are assumed to be products of hydrogenic wave functions of a given Z. However, for low-Z atomic systems, screening effects in autoionizing states are relatively much more important than for large-Z systems making the above argument invalid. For the atomic systems considered in this work, Table III shows that the autoionizing width is an increasing function of Z with two exceptions, the $[1s\,(2s\,2p)^3P]^2P^o$ and $[(1s\,2s)^3S\,3p]^2P^o$.

TABLE III. Energy and width for the lower ^2S, $^2P^o$, and ^2D resonances of Li I, Be II, B III (in a.u.). For notation see text. The results for $(1s\,2s\,2s)^2S$ in Ref. 3.

Resonance	E_{sp}	L	N	q	$10^3\langle H_1+H_2\rangle$	$10^5\langle H_3\rangle$	$10^6\langle H_4\rangle$	$10^5\langle H_5\rangle$	$10^4\Delta$	E total	$10^3\Gamma_e$	$10^7\Gamma_r$
$(1s\,2p\,2p)^2S$												
Be II	−9.699517	16	118	3.84	−1.8427	0.63	3.36	−1.869	2.266	−9.701112	0.210	8.769
B III	−15.741853	13	104	4.78	−4.6079	2.18	8.73	−3.38	2.798	−15.746105	0.2498	29.753
$[(1s2s)^3S\,3s]^2S$												
Li I	−5.199641	13	91	2.45	−0.6153	0.10	0.006	0.157	0.167	−5.200237	0.2900	
Be II	−9.584848	9	98	3.53	−2.0172	0.60	0.26	−0.294	−0.075	−9.586867	0.3655	0.069
B III	−15.338502	9	76	4.57	−5.0791	1.48	0.41	−0.315	0.725	−15.343493	0.5436	0.493
$[(1s2s)^1S\,3s]^2S$												
Be II	−9.500625	8	87	3.54	−1.8994	3.96	−0.66	0.591	0.407	−9.502444	0.235	4.045
B III	−15.220761	10	87	4.54	−4.6973	9.30	−1.32	0.894	0.846	−15.225285	0.312	12.738
$[1s(2s2p)^3P]^2P^o$												
Li I	−5.312761	26	110	2.47	−0.5900	0.63	−0.49	0.981	2.836	−5.313056	0.1364	
Be II	−9.960080	26	121	3.47	−1.9581	2.45	−2.08	2.35	3.758	−9.961635	0.1500	20.415
B III	−16.106000	15	101	4.45	−4.9541	6.22	−5.43	3.914	4.162	−16.110491	0.1488	67.377
$[1s(2s2p)^1P]^2P^o$												
Li I	−5.256864	13	108	2.52	−0.5802	0.42	0.67	−0.845	−0.2145	−5.257464	0.3679	
Be II	−9.878065	20	119	3.55	−1.9193	1.48	2.63	−2.331	−0.4951	−9.880016	0.7719	1.924
B III	−16.000739	16	105	4.60	−4.8681	6.37	6.32	−3.870	1.422	−16.005377	1.1245	7.837
$[(1s2s)^3S\,3p]^2P^o$												
Li I	−5.183387	8	93	2.46	−0.6108	0.04	0.001	0.071	0.040	−5.183993	0.00631	
Be II	−9.565456	15	100	3.48	−1.9920	0.22	−0.02	0.254	0.095	−9.567433	0.0118	4.268
B III	−15.309150	14	110	4.56	−4.9796	0.62	0.05	0.372	0.358	−15.314083	0.0140	13.295
$[(1s2s)^1S\,3p]^2P^o$												
Be II	−9.472140	16	113	3.54	−1.8714	2.17	0.84	−0.76	0.713	−9.473917	0.015	3.196
B III	−15.176379	14	110	4.56	−4.6638	5.55	1.92	−1.32	1.188	−15.180863	0.0078	11.074
$[(1s2p)^3P\,3s]^2P^o$												
Be II	−9.445095	12	108	3.52	−1.8902	1.69	0.89	−0.904	1.56	−9.446812	0.174	2.889
B III	−15.136901	11	110	4.52	−4.5650	4.04	5.70	−3.627	1.61	−15.141244	0.416	8.391
$(1s\,2p\,2p)^2D$												
Li I	−5.233703	17	110	2.35	−0.5599	0.081	0.871	−1.946	0.0727	−5.234200	0.4043	
Be II	−9.825287	17	111	3.18	−1.8189	0.42	3.12	−3.600	1.551	−9.826952	1.0129	9.679
B III	−15.918753	14	103	4.40	−4.5431	1.24	7.36	−5.43	3.879	−15.922876	1.5449	30.974
$[(1s2s)^3S\,3d]^2D$												
Li I	−5.166023	10	76	2.52	−0.6121	0.01	0.01	0.145	0.1385	−5.166619	0.0409	
Be II	−9.524384	13	74	3.49	−2.0007	0.07	−0.02	0.251	0.220	−9.526359	0.0612	0.972
B III	−15.245587	11	78	4.49	−4.9779	0.22	0.05	−0.164	0.330	−15.250531	0.081	3.352
$[(1s2s)^1S\,3d]^2D$												
Be II	−9.432790	13	86	3.54	−1.8552	2.56	−0.56	1.336	0.115	−9.434600	0.003	5.060
B III	−15.116553	11	85	4.55	−4.6191	6.81	−0.79	−1.078	0.12	−15.121111	0.008	19.143

TABLE IV. Radiative dipole transition probabilities from the $^2P^o$ resonances of B III (in sec^{-1}).[a]

Initial / Final	$[1s(2s2p)^3P]^2P^o$	$[1s(2s2p)^1P]^2P^o$	$[(1s2s)^3S\,3p]^2P^o$	$[(1s2s)^1S\,3p]^2P^o$	$[(1s2p)^3P\,3s]^2P^o$
$(1s\,1s\,2s)^2S$	2.7682(11)	3.1172(10)	4.9202(10)	1.5192(10)	6.2730(8)
$(1s\,1s\,3s)^2S$	7.8368(8)	1.8546(8)	1.3607(9)	1.8230(10)	2.9830(10)
$(1s\,1s\,4s)^2S$	1.2287(8)	4.6278(7)	3.2473(7)	3.9444(8)	7.4480(7)
$(1s\,2s\,2s)^2S$	1.3476(7)	5.7464(8)	3.9097(9)	6.9229(8)	2.8534(8)
$(1s\,2p\,2p)^2S$			2.5756(7)	1.2438(8)	2.3709(8)
$[(1s\,2s)^3S\,3s]^2S$			1.5927(6)	6.9397(7)	8.0798(7)
$[(1s\,2s)^1S\,3s]^2S$				3.2466(6)	9.8034(6)
$(1s\,1s\,3d)^2D$	6.6771(8)	3.1708(8)	5.2390(6)	1.0128(10)	2.3706(9)
$(1s\,1s\,4d)^2D$	1.2751(8)	1.0271(8)	9.8539(5)	1.6322(8)	4.8264(8)
$(1s\,2p\,2p)^2D$			4.1949(8)	6.4479(8)	3.1279(8)
$[(1s\,2s)^3S\,3d]^2D$				3.1891(6)	1.4416(5)
$(1s\,2p\,2p)^2P$			7.2436(5)	1.3607(8)	3.7784(8)
$[(1s\,2p)^3P\,3p]^2P$					8.2739(4)
Total	2.7853(11)	3.2399(10)	5.4959(10)	4.5780(10)	3.4689(10)

[a]Transition probabilities from other resonances will be supplied upon request.

III. COMPARISON WITH THEORY AND EXPERIMENT

In Table V we compare our results for the autoionization widths with other theoretical calculations and experiments. These results are given in meV. The conversion factors used for Li I, Be II, and B III are 27 209.48 meV/au, 27 209.95 meV/au, and 27 210.25 meV/au, respectively.

For the $[1s(2s2p)^3P]^2P^o$ state in Be II the experimental result of Cederquist et al.[2] is 4.58±0.13 meV; our result 4.08 meV is 11% less than this. The width which was measured experimentally and fitted to a Lorentzian profile was 4.67±0.12 meV; after subtracting from this the radiative widths of the upper and lower states in the $(1s2p2p)^2P \rightarrow [1s(2s2p)^3P]^2P^o$ transition, the result 4.58±0.13 meV was obtained. Our result for the radiative width of $(1s2p2p)^2P$ is 0.0858 meV (Ref. 7) and for the $[1s(2s2p)^3P]^2P^o$ state, 0.0555 meV (Ref. 8) which gives a combined result of 0.14 meV. This is larger than the estimate, 0.09 meV, based on theory given by Cederquist et al.[2] Another factor which could complicate the experimental analysis is the fine-structure splittings. For Be II we find the splittings of $(1s2p2p)^2P_{1/2,3/2}$ and $[1s(2s2p)^3P]^2P^o_{1/2,3/2}$ to be 2.31 meV (Ref. 7) and 1.61 meV which gives a spread of 2.5 Å in the 2831 Å region. This splitting is too small to be resolved in the experiment. However, when this theoretical fine structure is taken into account in the experimental analysis the width is reduced to 4.08 meV (Ref. 14) in good agreement with the saddle-point complex-rotation result.

The width of Li$[1s(2s2p)^3P]^2P^o$ was measured to be 2.6±0.13 meV from the $(1s2p2p)^2P \rightarrow [1s(2s2p)^3P]^2P^o$ transition.[1] This result is not corrected for the radiative widths of the upper and lower states since these corrections are expected to be small in lithium. Our result for the width of this resonance is 3.71 meV. It is 43% larger than the measured width. For lithium the fine-structure splittings of the upper and lower states are calculated in

this work to be 0.31 and 0.30 meV for the $(1s2p2p)^2P$ and $[1s(2s2p)^3P]^2P^o$ states, respectively. This splitting, being relatively much smaller, should not affect the analysis of the measured width by much.

For the $(1s2p2p)^2D$ state of Li, the experiment of Mannervik et al.[1] measures a width of 10.4±0.26 meV; our result, 11.00 meV, is 5.8% larger. For the same state in Be II Cederquist et al.[2] measure the width to be 30.3±1.1 meV; our result 27.56 meV is smaller by 9%. These experimental widths obtained from the transitions $[(1s2p)^3P\,3d]^2D^0 \rightarrow (1s2p2p)^2D$ in Li and Be II are not adjusted for the radiative widths of the upper and lower states. For the Be II transition we calculate the radiative widths for $[(1s2p)^3P\,3d]^2D^o$ and $(1s2p2p)^2D$ to be 0.001 39 meV (Ref. 7) and 0.026 34 meV (Ref. 8), respectively. The combined result, 0.028 meV, is indeed beyond the spectral resolution. The fine-structure splittings of the $[(1s2p)^3P\,3d]^2D^0$ and $(1s2p2p)^2D$ states are calculated to be -0.012 meV (Ref. 7) and -2.735 meV, respectively, for Be II, and -0.041 and -0.681 meV, respectively, for Li. These splittings are probably too small to affect the experimental analysis.

The agreement among the various theoretical results is poor. In Bhatia's calculations,[15] the closed-channel wave function is a configuration-interaction function derived from the quasiprojection operator technique. For the open-channel he uses a scattering function computed from the static exchange approximation with a closed-shell target state. With these wave functions he computed the width with the golden-rule formula. Although the widths of $(1s2s2s)^2S$, $[(1s2s)^3S\,3s]^2S$, and $[1s(2s2p)^1P]^2P^o$ in Ref. 15 agree reasonably well with ours, the widths for other states differ very substantially. For $[1s(2s2p)^3P]^2P^o$ of Li I, Be II, and B III his results are approximately twice ours. For Li$(1s2p2p)^2D$ his result is approximately half of ours. For Be II$(1s2p2p)^2D$ there is about a 20% difference between the two results.

All of the theoretical results for Li$[1s(2s2p)^3P]^2P^o$ are too large as compared to experiment. The closest result is

TABLE V. Comparison of autoionization widths in Li I, Be II, and B III (in meV).

	Li I	Be II	B III
$(1s\,2s\,2s)^2S$	36.84[a] 40.3[b]	52.99[a] 53[b] 83;23[c] 20.5[d] 92.93[e]	62.19[a] 68[b]
$(1s\,2p\,2p)^2S$		5.71[a] 8[b]	6.70[a] 9[b]
$[(1s\,2s)^3S\,3s]^2S$	7.89[a] 13[b]	9.95[a] 8[b]	14.79[a] 13[b]
$[1s\,(2s\,2p)^3P]^2P^o$	3.71[a] 7[b] 8.49;5.13;3.42[f] 5.07[h] 3.9[i] 3.07[j] 2.6±0.13[k]	4.08[a] 10[b] 12.8;5.46;4.31[g] 4.58±0.13[l] 4.08±0.11[m]	4.05[a] 10[b]
$[1s\,(2s\,2p)^1P]^2P^0$	10.01[a] 11[b] 11[i]	21.00[a] 17[b]	30.60[a] 28[b]
$[(1s\,2s)^3S\,3p]^2P^o$	0.172[a] 0.021[b]	0.321[a] 0.022[b]	0.381[a] 0.051[b]
$(1s\,2p\,2p)^2D$	11.00[a] 5[b] 21.5;17.2;10.0[f] 23[h] 123[j] 10.4±0.26[k]	27.56[a] 23[b] 40.4;38.2;31.3[g] 30.3±1.1[l]	42.04[a] 27[b]
$[(1s\,2s)^3S\,3d]^2D$	1.11[a] 0.75[b];0.89[m]	1.67[a] 2[b]	2.2[a] 3[b]
$[(1s\,2s)^1S\,3d]^2D$		0.08[a] 0.18[b]	0.2[a] 0.25[b]

[a]This work.
[b]Bhatia, Ref. 15.
[c]Nicolaides et al., Ref. 19.
[d]Palmquist et al., Ref. 22.
[e]Kelly, Ref. 23.
[f]Nicolaides et al., Ref. 20 (see text).
[g]Nicolaides et al., Ref. 21 (see text).
[h]Propin, Ref. 17.
[i]Manson, Ref. 18.
[j]Safronova et al., Ref. 16.
[k]Mannervik et al., Ref. 1.
[l]Cederquist et al., Ref. 2.
[m]Private communication, Ref. 14.

3.07 meV of Safranova et al.;[16] however, their width for Li$(1s\,2p\,2p)^2D$, 123 meV, is 12 times that of the experiment. Safronova et al. use a Z-dependent perturbation theory as does Propin.[17] Manson[18] used a perturbation-theory technique, in which the closed-channel wave function must be a Hatree-Fock function with no configuration interaction. A golden-rule-type formula yields a width of 3.9 meV for this lowest $^2P^o$ resonance. He also computes the width of the second lowest $^2P^o$ resonance and obtains 11 meV, in good agreement with the present result of 10 meV and with Bhatia's[15] result of 11 meV.

Nicolaides and collaborators[19−21] have published results for the resonances that have been measured experimentally. They calculate the width with a modified golden-rule formula.[20] The three results quoted for each state correspond to calculations with closed-channel wave functions of increasing complexity. The open-channel or final-state wave function in each calculation is the same, a Hartree-Fock wave function. As an example, the first result of Nicolaides et al.[20] for Li$[1s\,(2s\,2p)^3P]^2P^o$ corresponds to the use of a Hartree-Fock initial-state wave function for the $[1s\,(2s\,2p)^3P]^2P^o$ state, this gives a width of 1.45 meV. However, since their initial- and final-state wave functions are obtained independently of each other, they are not

TABLE VI. Transition wavelengths for $(1s\,2p\,2p)^2P \rightarrow [1s\,(2s\,2p)^3P]^2P^o$ and $[(1s\,2p)^3P\,3d]^2D^o \rightarrow (1s\,2p\,2p)^2D$. (Energy in a.u., wavelengths in Å, conversion factors: 455.669 Å/a.u. for Li and 455.661 Å/a.u. for Be II).

	State	$E^a_{\text{rel,sp}}$	This work E^b_{tot}	λ^c_{sp}	λ^d_{res}	λ Experiment	Bhatia[g]	Other theory[j] Nicolaides and collaborators
	$(1s\,2p\,2p)^2P$	$-5.214\,064$						
				4589.96	4603.10	4585[e]	4687.2	4898[h]
Li	$[1s\,(2s\,2p)^3P]^2P^o$	$-5.313\,340$	$-5.313\,056$					
	$[(1s\,2p)^3P\,3d]^2D^o$	$-5.089\,701$						
				3151.85	3153.44	3144[e]	3239.4	3232[h]
	$(1s\,2p\,2p)^2D$	$-5.234\,273$	$-5.234\,200$					
	$(1s\,2p\,2p)^2P$	$-9.801\,189$						
				2833.33	2839.97	2831.7[f]	2890.5	2975.07[i]
Be II	$[1s\,(2s\,2p)^3P]^2P^o$	$-9.962\,011$	$-9.961\,635$					
	$[(1s\,2p)^3P\,3d]^2D^o$	$-9.417\,771$						
				1113.17	1113.59	1112.3 ± 0.4[f]	1136.7	1169.69[i]
	$(1s\,2p\,2p)^2D$	$-9.827\,107$	$-9.826\,952$					

[a]Saddle-point energy or Rayleigh-Ritz energy plus relativistic and mass polarization corrections.
[b]Shifted included, i.e., $E_{\text{tot}} = E_{\text{rel,sp}} + \Delta$.
[c]Using $E_{\text{rel,sp}}$ for the autoionizing state.
[d]Using E_{tot} for the autoionizing state.
[e]Mannervik et al., Ref. 1
[f]Cederquist et al., Ref. 2.
[g]Bhatia, Ref. 15.
[h]Nicolaides et al., Ref. 20.
[i]Aspromallis et al., Ref. 21.
[j]Using the upper-state energy of this work. Relativistic and mass polarization corrections for the resonances are also included.

orthonormal. When they take into account this nonortho-normality the width becomes 8.49 meV. If a five configuration multiconfiguration Hartre-Fock (MCHF) function for $[1s\,(2s\,2p)^3P]^2P^o$ with energy $-5.299\,91$ a.u. is used and nonorthonormality is taken into account the width becomes 5.13 meV. If further correlations are added to the MCHF wave function the energy becomes -5.3066 a.u. At this point, taking into account nonorthonormality becomes computationally tedious and only the most important nonorthonormality contributions were taken into account with the final result of 3.42 meV for the width.

The width results of Nicolaides and collaborators[19-21] for $[1s\,(2s\,2p)^3P]^2P^o$ and $(1s\,2p\,2p)^2D$ in Li I and Be II are in reasonable agreement with our results. However, their $(1s\,2s\,2s)^2S$ width is very different from ours. We note that while their width fluctuates greatly in the various steps of their calculation, the width in our calculation appears to be more stable (see next section). Their final calculated energy position deviates substantially from the experiment (see Table VI).

In Table VI the wavelengths calculated in this work for the $(1s\,2p\,2p)^2P \rightarrow [1s\,(2s\,2p)^3P]^2P^o$ and $[(1s\,2p)^3P\,3d]^2D^0 \rightarrow (1s\,2p\,2p)^2D$ transitions in Li I and Be II are compared with those of experiment and other theory. The energies quoted for $(1s\,2p\,2p)^2P$ and $[(1s\,2p)^3P\,3d]^2D^o$ of Be II which include relativistic and mass polarization corrections were computed in an earlier work.[7] The energies quoted for the same two states in lithium are calculated

here. For the $(1s\,2p\,2p)^2P$ and $[(1s\,2p)^3P\,3d]^2D^o$ states of lithium we obtain the nonrelativistic energies $-5.213\,517$ a.u. and $-5.089\,141$ a.u., respectively. The calculated relativistic and mass polarization corrections are $-0.000\,547$ and $-0.000\,561$ a.u. for the two states. By adding these corrections to the energy, we obtain the results quoted in Table VI.

In the recent optical emission spectroscopy measurements, Lorentzian line profiles are assumed with the effect of the open-channel continuum neglected.[24,25] If this effect is neglected in the theoretical calculation, the energy will be simply the saddle-point energy. In Table VI two theoretical wavelengths for each transition are quoted from this work; one is calculated with the resonance energy and the other is calculated with the saddle-point energy (with relativistic and mass polarization corrections included). It appears that the nonshifted saddle-point energy gives a closer agreement with that of the experiment.

The calculated wavelengths are slightly too long as compared with the experimental results of Refs. 1 and 2 which indicates that the calculated energy for the autoionizing levels is too high. This follows from the fact that the energy of the upper states which are metastable against autoionization satisfy the upper bound principle and therefore should not be expected to be calculated too low. If we use $E_{\text{rel,sp}}$ to calculate λ and if we assume that the upper-state energies are accurate (judging from the comparison between theory and experiment in Ref. 7) then

the discrepancy with the experimental wavelengths implies that the energy of $[1s(2s2p)^3P]^2P^o$ of Li and Be II is too high by about 0.000 095 a.u. and that the energy of $(1s2p2p)^2D$ of Li and Be II is too high by approximately 0.000 34 a.u. This deficiency in energy is not surprising when one considers the number of partial waves necessary to account for the electron correlation in an autoionizing state (see Table I).

Also given in Table VI are the theoretical transition wavelengths obtained by using the nonrelativistic resonance energies of Bhatia[15] and of Nicolaides and collaborators.[20,21] In order to make a meaningful comparison with these references we have added our relativistic and mass polarization corrections to their nonrelativistic resonance energies. The transition energies quoted for these references were computed using the upper-state energies of Table VI. We note that although the width results of Nicolaides and collaborators are in reasonable agreement with our results, their transition wavelengths and therefore resonance energies are quite different from our results.

IV. CONVERGENCE OF THE WIDTH OF Li[$1s(2s2p)^3P]^2P^o$

In view of the poor comparison between our result and experiment for the width of Li[$1s(2s2p)^3P]^2P^o$ a detailed study of the convergence is needed to access the reliability of our theoretical result. In this work, we examined the convergence of this width with respect to both the open- and closed-channel components of our wave function.

The convergence was examined with respect to two different aspects of the open-channel: (a) the accuracy of the $(1s1s)^1S$ Li II target state, and (b) the number of U_k^L's used to represent the scattered electron. When carrying out these calculations, the same closed-channel basis functions were used as those in Table III.

The crudest target state possible is a one-term closed-shell target state. For this we used a product of two hydrogenic $1s$ orbitals with the effective nuclear charge set equal to the optimized value $Z - \frac{5}{16} = 2.6875$.[26] The energy of this target state is $-7.222 656$ a.u. With this target state and 15 U_k^L's we obtain 4.10 meV for the width. If the target state is improved by using a four-term $(s,s)^1S$ partial wave with energy $-7.251 861$ a.u. and the same number of U_k^L's are used, then the width becomes 3.85 meV. After the target state is improved further by adding to it a three-term $(p,p)^1S$ partial wave [so that the $(1s1s)^1S$ energy becomes $-7.274 796$ a.u.], the width reduces to 3.73 meV. Finally the addition of a one-term $(d,d)^1S$ partial wave results in our final three-partial-wave eight-term target state with energy $-7.276 970$ a.u. which yields a converged width of 3.71 meV. These computations indicate that accounting for electron correlation in the target state results in a 10% decrease in the width. Many theoretical calculations in the literature do not include any correlation in their target states.

To examine the convergence of the width with respect to the number of U_k's used for the scattered electron, we

performed calculations using the three-partial-wave eight-term target state with 11, 12, 13, 14, and 15 U_k's. The resulting fluctuation in the width occurred at the fifth significant digit, i.e., the result given in Tables III and V remained stable.

The convergence of the width with respect to the closed-channel was tested in three different ways: (a) with respect to the size of the closed-channel wave function; (b) with respect to the type of basis functions used to describe the closed-channel; and (c) fixing the closed-channel wave function before the complex rotation by forcing the C_j in Eq. (2) to be equal to the B_j of Eq. (3). When carrying out these calculations, the three-partial-wave eight-term target state with 15 U_k's was used for the open channel.

First, we calculate the width by using a limited number of terms in the closed-channel component. To this end we calculated a 14-term eight-partial-wave saddle-point wave function with energy $-5.307 433$ a.u. By using the 14 basis functions resulting from this calculation in Eq. (2) and then carrying out the complex-rotation computation of Eq. (6) a converged width of 4.276 meV is obtained. This is 15% larger than our result in Tables III and V. The shift from the saddle-point energy is 0.000 316 a.u. which is larger than that of Table III as should be expected. The convergence of the width with respect to angular correlations is demonstrated in Table VII for two cases. The first column corresponds to the use of the small closed-channel function discussed here. The second column results from using the large closed-channel basis of Table I. Both calculations converge at about the same rate with respect to the addition of angular correlations. The difference between the two columns results from the extra radial correlation obtained with the larger basis set.

A second test of the stability of our result for the width can be made by using the same closed-channel basis functions as those for the $[1s(2s2p)^1P]^2P^o$ and $[(1s2s)^3S3p]^2P^o$ states in Eqs. (2) and (6). The converged results using these (inferior) basis functions are 3.40 and 3.53 meV, respectively. These results are only 8% and 3% smaller than the result of Table III. This relatively small change in the width resulting from such a large change in the closed-channel basis functions seems to indicate that the width is very stable and it is not likely to change much by further improving our wave function.

One advantage of the wave function given by Eq. (2) as compared to many other theoretical calculations is its ability to account for the coupling between closed and open channels. The open-channel component can modify the closed-channel component through the C_j in the

TABLE VII. Convergence of the Li[$1s(2s2p)^3P]^2P^o$ width with respect to angular correlations (in meV).

Angular correlations included	Small closed-channel basis set	Large closed-channel basis set
ssp	5.080	4.660
spd + ssp	4.185	3.508
ppp + spd + ssp	4.302	3.709
sdf + ppp + spd + ssp	4.276	3.713

complex-rotation computation. Likewise, the closed channel can modify the open channel through the D_k. In many other theoretical width calculations, closed- and open-channel components or initial- and final-state wave functions are obtained from separate calculations with the result that these wave functions are fixed separately. The width is then computed by calculating a transition matrix element between these two wave functions.

As an alternative to the wave function given by Eq. (2) we could choose the following trial wave function for the complex-rotation computation:

$$\Psi(^2L) = a \Psi_{sp}(R_3 e^{i\theta}, \Omega_3)$$
$$+ A \sum_k D_k \psi_g(R_2 e^{i\theta}, \Omega_2) U_k^L(\mathbf{r}) , \qquad (9)$$

where Ψ_{sp} is the saddle-point wave function and a is a single linear variational parameter. In this case we have forced the C_j of Eq. (2) to be equal to the B_j of Eq. (3). When this wave function is used in Eq. (6) a width of 3.90 meV is obtained which is 5% larger than that obtained with Eqs. (2) and (6).

The most distinctive feature of the saddle-point technique is that it considers vacancy orbitals different from particle orbitals and that the vacancy orbitals are obtained by maximizing the energy of the innershell vacancy state. This is different from the frozen-core Hartree-Fock method[27] and other hole-projection techniques.[28] To what extent is this vacancy orbital more "correct" is not entirely clear. In this work, we wish to examine and compare results from different vacancy orbitals obtained with and without this maximization process.

Another point of interest is that in scattering theory, the Hilbert space is conveniently divided into a closed-channel and an open-channel subspace.[29] The two subspaces are assumed to be mutually orthogonal. For two-electron systems, the projection operators which project the total wave function into such subspaces are well defined.[30] However, for systems with three or more electrons, rigorous projection operators are not available.[31] Although the concept of closed and open channels is still extensively utilized in scattering theory, the orthogonality between these components is no longer obvious. On the other hand, if there is substantial overlap between the closed- and open-channel components, then the identification of such subspaces becomes less meaningful. In the saddle-point technique, the closed-channel wave function is obtained by building the proper vacancy into the wave

function. Whether this wave function will be orthogonal to the open channel has not been explicity investigated.

To answer these questions we present the results in Table VIII using the Li$[1s(2s\,2p)^3P]^2P^o$ calculation as an example. Here the closed-channel wave functions are 110 term functions obtained with Eqs. (3) and (4). In addition to the saddle-point wave function used earlier with $q=2.47$, we also obtain wave functions with $q=2$, 2.6875, and 3. The wave function with $q=2.6875$ bears some similarity to that of the quasiprojection operator method.[15] The energies of these wave functions are designated E_q in the table.

Two separate sets of calculations using Eq. (6) are presented in this table. In the first calculation Eq. (9) is used to calculate the resonance energy and width. The second calculation is obtained by using the wave function given by Eq. (2). The overlap given in this table is defined by

$$\left| \frac{\langle \Psi_{open} | \Psi_{closed} \rangle}{\langle \Psi_{tot} | \Psi_{tot} \rangle} \right| , \qquad (10)$$

where Ψ_{open} and Ψ_{closed} are obtained after the complex-rotation procedure.

One interesting feature in this table is that the resonance energies and widths in the second part all turn out to be very close. This is actually expected. With the large wave function used in these calculations, the basis set is "almost complete." In this case, the proper solution should appear based on the theory of the complex-rotation method.[9] However, the widths resulting from the use of Eq. (9) show clearly that a slightly inaccurate wave function could lead to erroneous results. This is particularly important when a golden-rule formula is used to compute the width. The fact that the shift for $q=2.47$ is at least 1 order of magnitude smaller than that of the other calculations in this table shows that the saddle-point energy is far more accurate.

Perhaps the most interesting feature of this table is the very small overlap between the open- and the closed-channel components of the wave function for $q=2.47$. This small overlap suggests that carrying out the saddle-point variation procedure results in a wave function that is essentially orthogonal to the open channel. In this case, the Hilbert space can easily be separated into closed- and open-channel components without the explicit construction of the corresponding projection operators. The over-

TABLE VIII. Comparison of shifts and widths obtained from the wave functions given by Eq. (9) and (2). $q=2.47$ is the optimized value from the saddle-point technique (in a.u.).

Ψ	From Eq. (9)					From Eq. (2)			
q	$-E_q^a$	$-E_{res}$	$10^2\Delta$	$10^4\Gamma$	Overlap[b]	$-E_{res}$	$10^2\Delta$	$10^4\Gamma$	Overlap[b]
2	5.348 206	5.296 655	5.1551	3.446	0.027 423	5.312 287	3.5919	1.337	0.011 968
2.47	5.312 761	5.312 475	0.0286	1.435	0.000 007	5.312 477	0.0284	1.364	0.000 007
2.6875	5.315 079	5.312 416	0.2663	1.735	0.000 674	5.312 510	0.2569	1.367	0.000 626
3	5.324 531	5.310 628	1.3903	2.884	0.005 426	5.312 539	1.1992	1.383	0.003 887

[a]Nonrelativistic energy given by the closed-channel part of the wave function.
[b]See Eq. (10) in text.

laps corresponding to the other q value in this table are orders of magnitude larger.

V. SUMMARY

In this work we have calculated the autoionization widths for eleven resonances in Li I, Be II, and B III. The results for the $[1s(2s2p)^3P]^2P^o$ and $(1s2p2p)^2D$ states in Li I and Be II are compared with the recent measurements. Reasonable agreement with experiment is obtained for the $(1s2p2p)^2D$ state in both Li I and Be II. For the $[1s(2s2p)^3P]^2P^o$ state very good agreement is obtained for Be II; however, the result for Li deviates substantially from that of the experiment. In order to examine closely the theoretical result for Li we have carried out detailed tests of the convergence of this width with respect to various aspects of the wave function used in this work. We find that our result is stable within the framework of the saddle-point complex-rotation method. The reason for this discrepancy with experiment is not clear at this point. Experimentally, a Lorentzian line profile has been assumed where the effect of the continuum is assumed to be negligible. It is not clear whether the continuum has made a significant contribution (via the line profile[24,25])

for the width of this state or whether some important effects have not been considered in our work.

On the experimental side, recently improved techniques in beam-foil spectroscopy have quoted measurements with resolutions of 1 Å in the 4000-Å region. This corresponds to an energy resolution of less than 1 meV. These precision measurements present a challenge to theoretical calculations of autoionizing states. The transition wavelengths computed in this work with saddle-point energies that include relativistic and mass polarization corrections indicate that the energies are still too high by a few meV when compared to the experiments of Refs. 1 and 2. It is conceivable that a more extensive configuration interaction calculation similar to those of Bunge and Bunge[32] on Li bound states may bring the saddle-point energy result even closer to that of the experiment.

ACKNOWLEDGMENTS

[1]S. Mannervik, H. Cederquist, and M. Kisielinski, Phys. Scr. **T8**, 107 (1984).

[2]H. Cederquist, M. Kisielinski, S. Mannervik, and T. Andersen, J. Phys. B **17**, 1969 (1984).

[3]B. F. Davis and K. T. Chung, Phys. Rev. A **29**, 1878 (1984).

[4]B. F. Davis and K. T. Chung, J. Phys. B **15**, 3113 (1982).

[5]K. T. Chung and R. Bruch, Phys. Rev. A **28**, 1418 (1983).

[6]K. T. Chung, Phys. Rev. A **23**, 2957 (1981); **24**, 1350 (1981).

[7]B. F. Davis and K. T. Chung, Phys. Rev. A **29**, 2586 (1984).

[8]B. F. Davis and K. T. Chung, J. Phys. B **17**, 4295 (1984).

[9]For a review, see Y. K. Ho, Phys. Rep. **99**, 1 (1983). Also B. R. Junker and C. L. Huang, Phys. Rev. A **18**, 313 (1978); B. R. Junker, *ibid.* **18**, 2437 (1978).

[10]K. T. Chung, Phys. Rev. A **20**, 1743 (1979); K. T. Chung and B. F. Davis, *ibid.* **22**, 835 (1980).

[11]C. L. Pekeris, Phys. Rev. **112**, 1649 (1958).

[12]K. T. Chung and B. F. Davis, Phys. Rev. A **26**, 3278 (1982).

[13]R. D. Cowan, *The Theory of Atomic Structure and Spectra* (University of California Press, Berkely, 1981), p. 589.

[14]T. Andersen and S. Mannervik (private communication).

[15]A. K. Bhatia, Phys. Rev. A **18**, 2523 (1978).

[16]U. I. Safronova and V. S. Senashenko, Opt. Spektrosk. **42**, 798 (1977) [Opt. Spectrosc. **42**, 462 (1977)]; J. Phys. B **11**, 2623 (1977).

[17]R. Propin, Opt. Spektrosk. **17**, 618 (1964) [Opt. Spectrosc. **17**,

332 (1964)].

[18]S. Manson, Phys. Rev. **145**, 35 (1966).

[19]C. A. Nicolaides, Y. Komninos, and D. R. Beck, Phys. Rev. A **27**, 3044 (1983).

[20]C. A. Nicolaides and G. Aspromallis, J. Phys. B **16**, L251 (1983).

[21]G. Aspromallis and C. A. Nicolaides, J. Phys. B **17**, L249 (1984).

[22]M. Palmquist, P. L. Altick, J. Richter, P. Winkler, and R. Yaris, Phys. Rev. A **23**, 1795 (1981).

[23]H. P. Kelly, Phys. Rev. A **9**, 1582 (1974).

[24]U. Fano, Phys. Rev. **124**, 1866 (1961).

[25]U. Fano and J. W. Cooper, Phys. Rev. **137**, A1364 (1965).

[26]E. Merzbacher, *Quantum Mechanics*, 2nd ed. (Wiley, New York, 1970), p. 445.

[27]See, for example, E. J. McQuire, in *Atomic inner-shell process*, edited by B. Crasemann (Academic, New York, 1975), Vol. I, p. 293.

[28]C. A. Nicolaides, Phys. Rev. A **6**, 2078 (1972).

[29]H. Feshbach, Ann. Phys. (N.Y.) **5**, 357 (1958); **19**, 287 (1962).

[30]Y. Hahn, T. F. O'Malley, and L. Spruch, Phys. Rev. **128**, 932 (1962).

[31]A. Temkin, A. K. Bhatia, and J. N. Bardsley, Phys. Rev. A **5**, 1663 (1972).

[32]C. F. Bunge and A. V. Bunge, Phys. Rev. A **17**, 816 (1978).